

三角柔性多羧酸金属有机骨架化合物的合成、结构及荧光性质

荣介伟^{1,2} 章文伟^{*2}

(¹ 淮南师范学院化学与材料工程学院, 淮南 232038)

(² 南京大学化学化工学院, 配位化学国家重点实验室, 南京 210023)

摘要: 以柔性 1,3,5-三(4-羧酸苯氧基)苯(H_3TCPB)为配体, 以 4,4'-联吡啶(4,4'-BPY)为辅助配体, 在溶剂热条件下合成了 2 个新颖的分别具有三核锌簇和三核钴簇的金属有机骨架化合物: $\{[Zn_3(TCPB)_2(4,4'-BPY)] \cdot DMF \cdot 3H_2O\}_n$ (**1**) 和 $\{[Co_{15}(TCPB)(DMF)(H_2O)] \cdot DMF\}_n$ (**2**), 通过单晶 X 射线衍射, 红外光谱, 元素分析, 热重分析和粉末 X 射线衍射对其结构进行了表征。单晶 X 射线衍射分析表明化合物 **1** 属于三斜晶系, $P\bar{1}$ 空间群, 表现出三维(3,8)连接的网状结构, 拓扑符号为: $\{4^3\}_2 \cdot \{4^6 \cdot 6^{18} \cdot 8^4\} \cdot \{6\}$; 化合物 **2** 也属于三斜晶系, $P\bar{1}$ 空间群, 为二维(3,6)连接的网络层状结构, 拓扑符号为: $\{4^3\}_4 \cdot \{4^6 \cdot 6^{18} \cdot 8^4\}$ 。此外, 荧光性质研究表明固态化合物 **1** 在室温条件下发射出源于 $TCPB^{3-}$ 和 4,4'-BPY 配体的淡蓝色荧光, 而化合物 **2** 在相似的条件没有荧光发射。

关键词: 柔性羧酸配体; 金属有机骨架化合物; 晶体结构; 荧光

中图分类号: O614.24¹; O614.81²

文献标识码: A

文章编号: 1001-4861(2018)12-2307-09

DOI: 10.11862/CJIC.2018.281

Syntheses, Structures and Photoluminescent Properties of Metal-Organic Frameworks Based on Triangle Flexible Multi-Carboxylic Ligand

RONG Jie-Wei^{1,2} ZHANG Wen-Wei^{*2}

(¹School of Chemical and Materials Engineering, Huainan Normal University, Huainan, Anhui 232038, China)

(²State Key Laboratory of Coordination Chemistry, School of Chemistry and Chemical Engineering, Nanjing University, Nanjing 210023, China)

Abstract: Two novel metal-organic frameworks $\{[Zn_3(TCPB)_2(4,4'-BPY)] \cdot DMF \cdot 3H_2O\}_n$ (**1**) with trinuclear zinc cluster units and $\{[Co_{15}(TCPB)(DMF)(H_2O)] \cdot DMF\}_n$ (**2**) with trinuclear cobalt cluster SBUs, have been prepared under solvothermal conditions based on flexible 1,3,5-tri(4-carboxyphenoxy)benzene ligand (H_3TCPB) with the help of ancillary bridging N-donor pyridyl linker 4,4'-bipyridine (4,4'-BPY), and characterized by single crystal X-ray diffraction, IR spectra, elemental analyses, thermogravimetric analyses (TGA) and powder X-ray diffraction (PXRD). The single crystal X-ray diffraction analysis reveals that complex **1** crystallizes in triclinic space group $P\bar{1}$ and exhibits three-dimensional (3D) (3,8)-connected network with Schläfli symbol of $\{4^3\}_2 \cdot \{4^6 \cdot 6^{18} \cdot 8^4\} \cdot \{6\}$, complex **2** also belongs to the triclinic system with space group of $P\bar{1}$ and shows two-dimensional (2D) (3,6)-connected net-like layered framework with Schläfli symbol of $\{4^3\}_4 \cdot \{4^6 \cdot 6^{18} \cdot 8^4\}$. In addition, the study of the solid state photoluminescent property of complex **1** indicates that it emits light blue fluorescence arising from $TCPB^{3-}$ and 4,4'-BPY ligands at room temperature, while complex **2** is non-emissive under similar conditions. CCDC: 1860924, **1**; 1865905, **2**.

Keywords: flexible carboxylic ligand; metal-organic framework; crystal structure; photoluminescence

收稿日期: 2018-08-30。收修改稿日期: 2018-10-23。

国家自然科学基金(No.21371091, 21371150)资助项目。

*通信联系人。E-mail: wwzhang@nju.edu.cn

0 Introduction

Over the past two decades, the metal-organic frameworks (MOFs) have received growing interest not only for their bewitching architectures^[1-2], but also for their potential applications in gas adsorption^[3-5], magnetism^[6], catalysis^[7-9], nonlinear optics^[10-11] and luminescence^[12-15]. Moreover, with respect to conventional metal-organic frameworks, luminescent MOFs have distinctive advantages owing to their widely potential applications such as light-emitting diodes, environmental probe, display devices, electro-chemical sensors and biomedicine^[16]. Photoluminescent property in MOFs commonly causes by the organic building components such as conjugated organic ligands and inorganic metal ions clusters with closed shell electron configuration^[17].

Among various conjugated organic ligands, owing to their natural characteristics, the tripodal rigid carboxylate ligands are promising candidates for constructing porous MOFs because of their abundant coordination modes to metal ions, allowing for various structural topologies^[18-19]. Recently, triangle flexible carboxylate ligands were used to build interesting metal-organic frameworks^[20-21], the flexibility of the triangle flexible carboxylate ligands provides the constructed functional MOFs tunable structures, which further affects the properties^[22-23]. Moreover, when the ancillary bridging pyridine linker is introduced to build the frameworks, the final structures have greater tenability because of its great effects on the final architectures and topology as well as coordination modes and molecular conformations of carboxylate acids^[24-27]. Although a lot of transition metal ions have been used to construct MOFs, the Zn-based MOFs are the most interested transition metal-based luminescent MOFs. MOFs based on d^{10} metal ions not only have various coordination geometries, but also display excellent luminescence behaviour with functional π -conjugated aromatic ligands^[28-29].

Herein, we selected the triangle flexible multi-carboxylic acid, namely, 1,3,5-tri(4-carboxyphenoxy)benzene ligand (H_3TCPB), and an ancillary bridging

pyridine linker, namely, 4,4'-bipyridine (4,4'-BPY) to synthesize two new metal-organic frameworks $\{[Zn_3(TCPB)_2(4,4'-BPY)] \cdot DMF \cdot 3H_2O\}_n$ (**1**) with trinuclear zinc cluster units and $\{[Co_{1.5}(TCPB)(DMF)(H_2O)] \cdot DMF\}_n$ (**2**) with trinuclear cobalt cluster SBUs, and studied their crystal structures and photoluminescent properties in detail.

1 Experimental

1.1 Materials and measurements

All reagents and materials are of analytical grade and used as received from commercial sources without further purification. The ligand 1,3,5-tri(4-carboxyphenoxy)benzene ligand (H_3TCPB) was prepared according to the literature procedure^[30]. Elemental analyses (C, H and N) were carried out on a Perkin-Elmer 240 analyzer. The IR spectra were obtained on a NICOLET iS10 spectrometer in the $4\ 000 \sim 500\ cm^{-1}$ region. Powder X-ray diffraction (PXRD) measurements using $Cu\ K\alpha$ ($\lambda=0.154\ 056\ nm$) radiation at room temperature (40 kV, 40 mA, Scanning range: $5^\circ \sim 50^\circ$) were carried out in air with a Bruker D8 Discover diffractometer. Thermal gravimetric analyses (TGA) were performed using a DTA-TGA 2960 thermogravimetric analyzer in nitrogen atmosphere with a heating rate of $10\ ^\circ C \cdot min^{-1}$ from 30 to 700 $^\circ C$. The luminescence spectra in the solid states were performed on RF-5301 PC fluorescence spectrometer at room temperature.

1.2 Synthesis

1.2.1 Synthesis of complex $\{[Zn_3(TCPB)_2(4,4'-BPY)] \cdot DMF \cdot 3H_2O\}_n$ (**1**)

A solution of $Zn(NO_3)_2 \cdot 6H_2O$ (6 mg, 0.02 mmol), H_3TCPB (5 mg, 0.01 mmol), 4,4'-BPY (2 mg, 0.013 mmol), DMF (0.5 mL) and H_2O (0.1 mL) were mixed and sealed in a 10 mL Teflon-lined autoclave and heated to 85 $^\circ C$ for 48 h. Colorless block-shaped crystals were obtained after gradually cooled to room temperature at a rate of $10\ ^\circ C \cdot h^{-1}$ (Yield: 75% based on Zn). Anal. Calcd. for $C_{67}H_{51}Zn_3N_3O_{22}$ (%): C, 55.64; H, 3.55; N, 2.91. Found(%): C, 55.45; H, 3.43; N, 2.63. Selected IR data (KBr pellet, cm^{-1}): 3 392 (b), 3 071 (w), 1 595 (s), 1 397 (s), 1 223 (s), 1 161 (s), 1 117 (s), 1 005 (s), 855 (m), 782 (s), 708 (m), 645 (m) (Supporting

Information, Fig.S1).

1.2.2 Synthesis of complex $\{[\text{Co}_{1.5}(\text{TCPB})(\text{DMF})(\text{H}_2\text{O})] \cdot \text{DMF}\}_n$ (**2**)

A solution of $\text{Co}(\text{NO}_3)_2 \cdot 6\text{H}_2\text{O}$ (6 mg, 0.02 mmol), H_3TCPB (5 mg, 0.01 mmol), DMF (0.4 mL) and H_2O (0.1 mL) were mixed and sealed in a 10 mL Teflon-lined autoclave and heated to 120 °C for 48 h. Light-pink block-shaped crystals were obtained after gradually cooled to room temperature at a rate of 5 °C $\cdot \text{h}^{-1}$ (Yield: 75% based on Co). Anal. Calcd. for $\text{C}_{33}\text{H}_{31}\text{Co}_{1.5}\text{N}_2\text{O}_{12}$ (%): C, 53.85; H, 4.25; N, 3.81. Found(%): C, 53.65; H, 4.45; N, 3.90. Selected IR data (KBr pellet, cm^{-1}): 3 427 (b), 2 942 (w), 1 677 (s), 1 657 (s), 1 631 (s), 1 594 (s), 1 412 (s), 1 222 (s), 1 161 (m), 1 110 (m), 1 003 (m), 791 (m) (Fig.S1).

1.3 Single crystal X-ray crystallography

Suitable single crystals of **1** and **2** were carefully selected under an optical microscope and glued to thin glass fibers. Single crystal X-ray diffraction data were collected on a Bruker Smart Apex II CCD

diffractometer at 296 K using graphite monochromated Mo $K\alpha$ radiation ($\lambda=0.071\ 073\ \text{nm}$). Data reductions and absorption corrections were performed with the SAINT^[31] and SADABS2^[32] software packages, respectively. Structure was solved by a direct method using the SHELXL-97 software package^[33]. The non-hydrogen atoms were anisotropically refined using the full-matrix least-squares method on F^2 . All hydrogen atoms were placed at the calculated positions and refined riding on the parent atoms. In complex **1**, solvent molecules in the structure were highly disordered and were impossible to refine using conventional discrete-atom models. To resolve this issue, the contribution of solvent electron density was removed by SQUEEZE routine in PLATON^[34].

The crystallographic data and details of structural refinements for **1** and **2** are listed in Table 1 and selected bond distances and angles are summarized in Table S1 and Table S2.

CCDC: 1860924, **1**; 1865905, **2**.

Table 1 Crystallographic data and structural refinements for **1** and **2**

Complex	1	2
Empirical formula	$\text{C}_{67}\text{H}_{51}\text{Zn}_3\text{N}_3\text{O}_{22}$	$\text{C}_{33}\text{H}_{31}\text{Co}_{1.5}\text{N}_2\text{O}_{12}$
Formula weight	1 446.28	736.01
Crystal system	Triclinic	Triclinic
Space group	$P\bar{1}$	$P\bar{1}$
a / nm	1.635(12)	1.019 26(8)
b / nm	1.661 81(12)	1.109 27(8)
c / nm	1.751 14(12)	1.612 08(12)
$\beta / (^\circ)$	83.104(10)	91.862(10)
V / nm^3	4.332 4(5)	1.664 1(2)
Z	2	1
$D_c / (\text{Mg} \cdot \text{m}^{-3})$	1.011	1.467
μ / mm^{-1}	0.875	0.822
$F(000)$	1 340	757
Reflection collected	21 208	5 808
Unique reflection	10 022	5 202
R_{int}	0.038 9	0.014 6
θ range for data collection / $(^\circ)$	1.336~28.275	1.271~25.008
GOF	1.146	1.104
$R_1^a, wR_2^b [I > 2\sigma(I)]$	0.057 1, 0.124 1	0.032 7, 0.112 1
R_1^a, wR_2^b (all data)	0.121 8, 0.147 9	0.036 8, 0.119 7

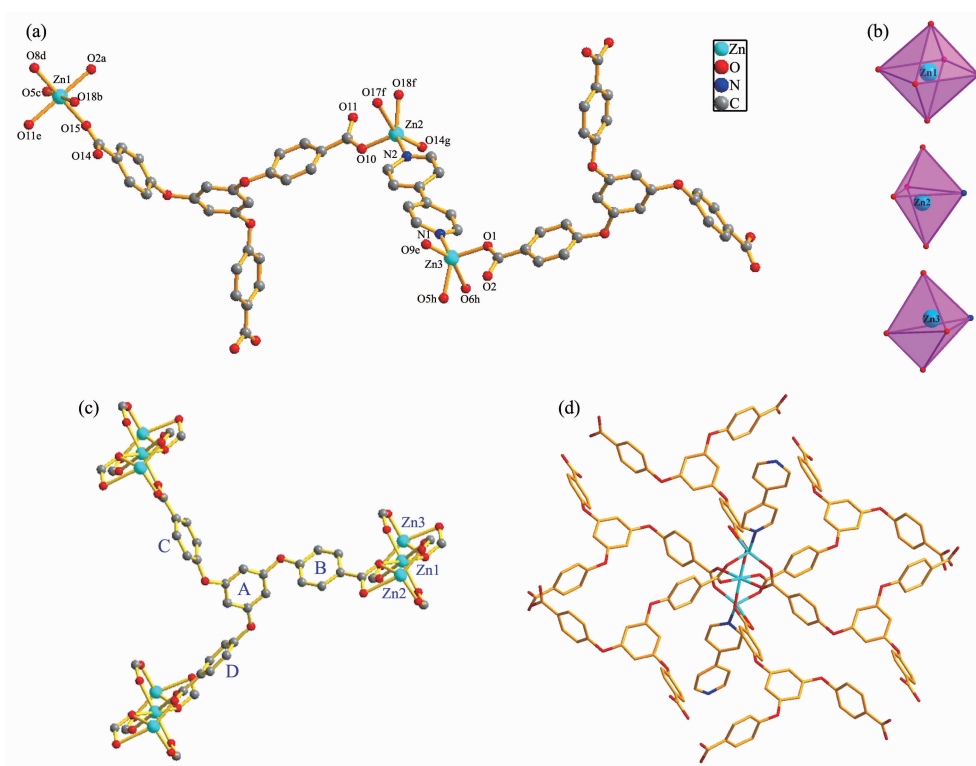
$$^a R_1 = \sum \|F_o\| - |F_c| / \sum \|F_o\|; ^b wR_2 = \{ \sum [w(F_o^2 - F_c^2)^2] / \sum [w(F_o^2)^2] \}^{1/2}$$

2 Results and discussion

2.1 Crystal structures

The powder X-ray diffraction (PXRD) experiments for complexes **1** and **2** were carried out carefully to check phase purity at room temperature. The patterns showed that the main peaks of the synthesized MOFs were closely consistent with those of the simulations from the single-crystal X-ray diffraction data, which imply high quality of the obtained products (Fig.S2). Crystal of **1** belongs to the triclinic space group $P\bar{1}$. As shown in Fig.1a, its asymmetric unit cell consists of three Zn^{2+} ions, two fully deprotonated TCPB $^{3-}$ ligands and one coordinated 4,4'-BPY molecule. Three crystallographically independent Zn^{2+} ions (labeled as Zn1, Zn2 and Zn3, respectively) are coordinated with oxygen atoms and nitrogen atom, exhibiting three different coordination geometries (Fig.1b). The Zn1...Zn2 distance is about 0.324 10(2) nm and the Zn1...Zn3 distance is about 0.325 90(2) nm. The Zn1 atom was

located in the center and bridged Zn2 and Zn3 atoms to form a trinuclear Zn cluster unit (Fig.1c). The Zn1 ion in the middle of the $[\text{Zn}_3(\text{CO}_2)_6]$ SBU is octahedron coordination geometry, encircled by six carboxylate oxygen atoms (O2a, O5c, O8d, O11e, O15 and O18b) from six different TCPB $^{3-}$ ligands to result in a $[\text{Zn}_3\text{O}_6]$ unit, while the other two asymmetry-related Zn2 and Zn3 ions both adopt a distorted trigonal bipyramid coordination geometry with a $[\text{Zn}_2\text{O}_4\text{N}]$ and $[\text{Zn}_3\text{O}_4\text{N}]$ unit, respectively (Fig.1b and Fig.S3), coordinated by four carboxylate oxygen atoms (O10, O14g, O17f and O18f for Zn2; O1, O5h, O6h and O9e for Zn3) from three different TCPB $^{3-}$ ligands, one nitrogen atom from the coordinated 4,4'-BPY molecule (N2 for Zn2; N1 for Zn3). The carboxylate groups in complex **1** adopt two kinds of coordination modes. One shows chelating and bridging modes to link two Zn ions, while the other two adopt a bidentate bridging coordination mode to coordinate with two Zn ions. The dihedral angles between the central benzene (A) and the three



Symmetry codes: a: $-1+x, y, -1+z$; b: $-1+x, 1+y, z$; c: $-1+x, -1+y, -1+z$; d: $-2+x, y, -1+z$; e: $-1+x, y, z$; f: $x, 1+y, z$; g: $1+x, y, z$; h: $x, -1+y, z$

Fig.1 (a) Coordination environments of Zn^{2+} ions with the H atoms omitted for clarity; (b) Coordination polyhedron of Zn^{2+} ions; (c) One TCPB $^{3-}$ ligand linking three $[\text{Zn}_3(\text{CO}_2)_6]$ SBUs; (d) One $[\text{Zn}_3(\text{CO}_2)_6]$ SBU connected by six TCPB $^{3-}$ ligands and two 4,4'-BPY linkers

benzene rings B, C and D are 75.839° , 69.199° and 69.139° , respectively, and the dihedral angles among the three benzene rings B and C, B and D, and C and D are 78.830° , 39.346° and 72.518° , respectively (Fig.1c). This dihedral data indicates that ligand TCPB^{3-} is extremely unsymmetrical. The dihedral angle between the two pyridyl rings is 30.961° . Therefore, two pyridyl rings of 4,4'-BPY are not coplanar. In **1**, each TCPB^{3-} ligand links three $[\text{Zn}_3(\text{CO}_2)_6]$ SBUs (Fig. 1c), each $[\text{Zn}_3(\text{CO}_2)_6]$ SBU is connected by six TCPB^{3-} ligands and two 4,4'-BPY ligands, and each 4,4'-BPY ligand links two $[\text{Zn}_3(\text{CO}_2)_6]$ SBUs by terminal nitrogen atoms (Fig.1d), such building units are repeated to form a three-dimensional (3D) network. As summarized in Table S1, the Zn-O bond lengths range from 0.193 5(2) to 0.232 1(3) nm, the bond distances of Zn-N are in the range of 0.202 4(3)~0.204 4(3) nm, and the O-Zn-O bond angles span from 56.97° to

179.37° , the coordination bond lengths and bond angles around the Zn ions are in good agreement with the reports^[35].

The guest DMF and water molecules, being disordered, locate in the channels. All DMF and water molecules can be completely removed upon heating, and there exist two types of one-dimensional channels along the *c* axis, which possess the open window of $1.205(2) \text{ nm} \times 0.860(3) \text{ nm}$ (A) and $1.815(3) \text{ nm} \times 1.760(3) \text{ nm}$ (B) when the van der Waals radii of the atoms at the wall of the channel are subtracted, respectively (Fig.2c). Moreover, open channel systems also exist along the *a* and *b* axis, with an open window size of $1.775(2) \text{ nm} \times 1.576(2) \text{ nm}$ and $1.441(2) \text{ nm} \times 1.350(3) \text{ nm}$, respectively (Fig.2a and 2b), and the solvent-accessible volume is about 46.2% calculated by PLATON/SOLV^[34] when the guest DMF and water molecules are removed (Fig.2 and Fig.S3).

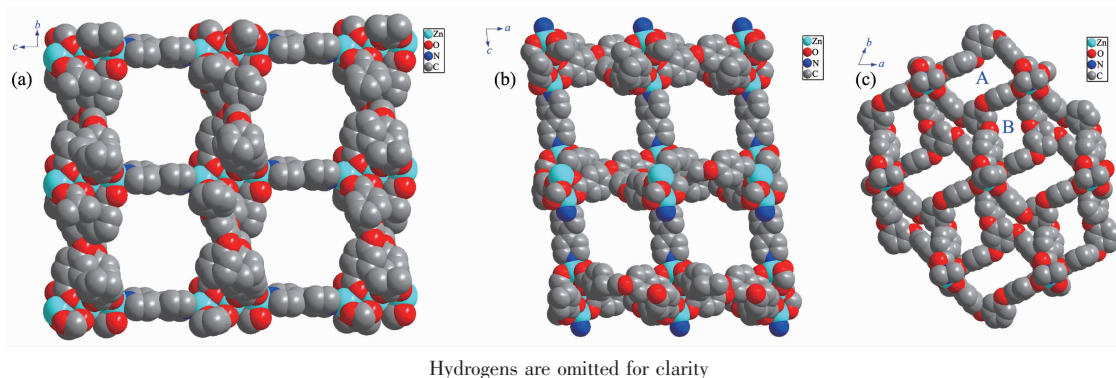
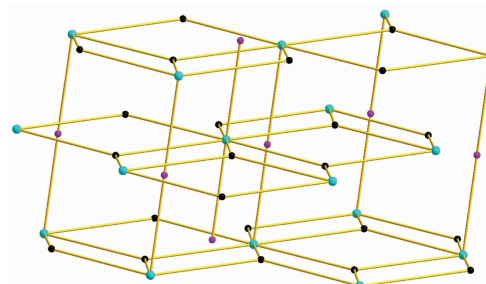


Fig.2 Space filled representation of the 3D framework in **1** viewed from *a*, *b*, and *c* directions

From the view point of topology, the 3D structure of **1** can be described as a (3,8)-connected network with Schlfl symbol of $\{4^3\}_2 \cdot \{4^6 \cdot 6^{18} \cdot 8^4\} \cdot \{6\}$ by considering each $[\text{Zn}_3(\text{CO}_2)_6]$ SBU as an 8-connected node and the organic ligand as a 3-connected node (Fig.3).

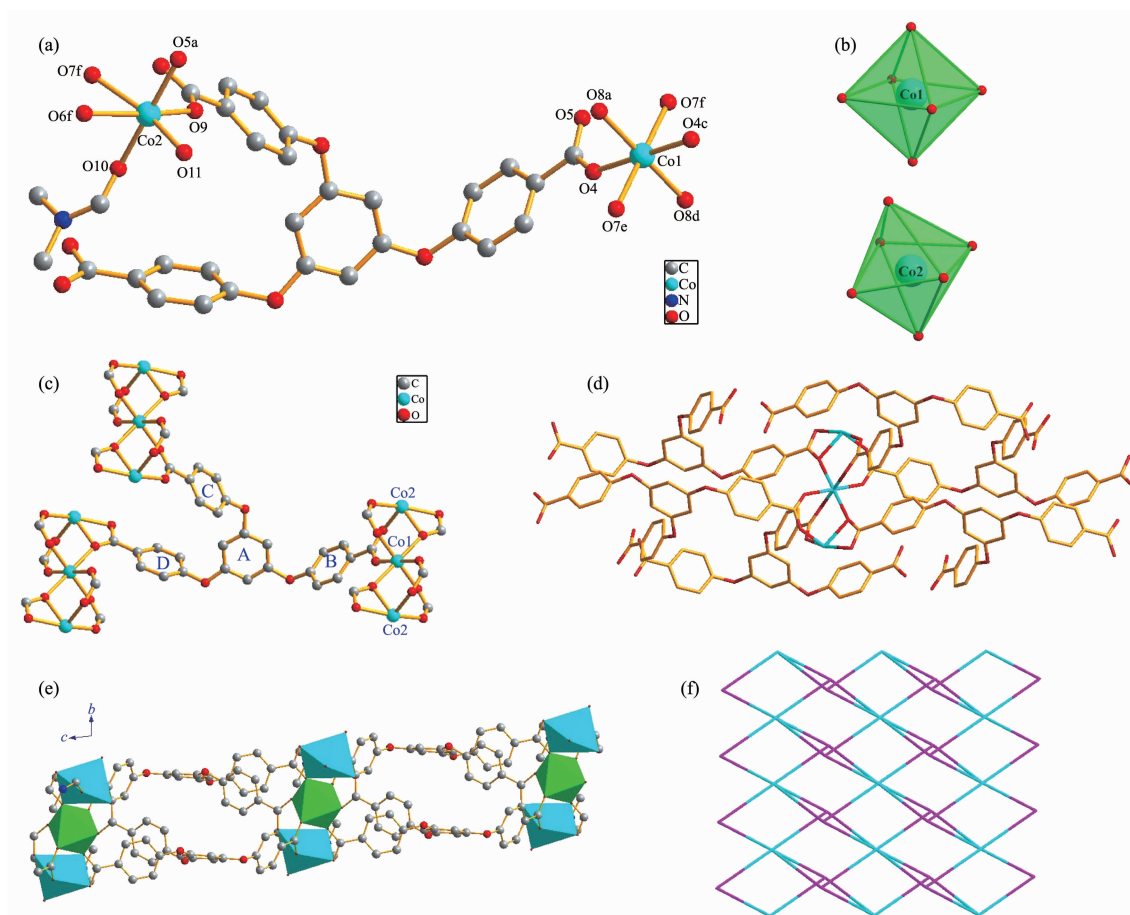
Single-crystal X-ray diffraction study reveals that complex **2** contains a two dimensional layer framework built by three-nuclear Co SBUs and three-connected TCPB^{3-} ligand. Crystal **2** belongs to the triclinic system with space group of $P\bar{1}$. As shown in Fig.4a, its asymmetric unit cell contains one and a half Co^{2+} ions, one fully deprotonated TCPB^{3-} ligand, one coordinated DMF molecule and one coordinated H_2O molecule. Two crystallographically independent Co^{2+} ions (labeled

as Co1 and Co2, respectively) exhibit different coordination geometries although they are both coordinated with six oxygen atoms (Fig.4b). The



Black dot: 3-connected node of TCPB^{3-} organic ligand, Pink dot: 2-connected linker of 4,4'-BPY, Turquoise dot: 8-connected node of SBU

Fig.3 (3,8)-connected network of **1**



Symmetry codes: a: $-x, 1-y, 1-z$; b: $-1+x, y, -1+z$; c: $-x, 1-y, -z$; d: $x, y, -1+z$; e: $1-x, 1-y, 1-z$; f: $1-x, 1-y, 2-z$; Green and turquoise polyhedra correspond to $[\text{Co}_{10}]_6$ and $[\text{Co}_{20}]_6$ units, respectively in (e); Purple represents the 3-connected node of organic ligand and turquoise represents the 6-connected node of SBU in (f)

Fig.4 (a) Coordination environments of Co^{2+} ions with the H atoms omitted for clarity; (b) Coordination polyhedron of Co^{2+} ions; (c) One TCPB^{3-} ligand linking three $[\text{Co}_3(\text{COO})_6]$ SBUs; (d) One $[\text{Co}_3(\text{COO})_6]$ SBU connected by six TCPB^{3-} ligands; (e) Polyhedral representation of **2** viewed from a direction; (f) (3,6)-connected network of **2**

coordination geometry around Co1 ions can be described as an octahedron with its six coordinated oxygen atoms coming from six different TCPB^{3-} ligands (O4, O4c, O7b, O7e, O8a and O8d), which results in a $[\text{Co}_{10}]_6$ unit. As for Co2 ions, they bond to four oxygen atoms (O5a, O6f, O7f and O9) from three TCPB^{3-} ligands, one oxygen atom (O10) from one DMF molecule and one oxygen atom (O11) from one H_2O molecule with a $[\text{Co}_{20}]_6$ unit, resulting in distorted octahedron geometries. As shown in Fig.4c and 4d, among the six coordinated TCPB^{3-} ligands, four carboxylates from four TCPB^{3-} coordinate to Co1 and Co2 as a bidentate bridging coordination mode, while the other two carboxylates from two different TCPB^{3-} ligands coordinate to Co1 and Co2 centers in a

chelating and bridging coordination mode to give a three-nuclear $[\text{Co}_3(\text{COO})_6]$ subunit (SBU) with $\text{Co1} \cdots \text{Co2}$ distance of 0.351 3(2) nm within this SBU. The dihedral angles between the central phenyl ring (A) and the three phenyl rings B, C and D are 70.93° , 73.73° and 80.89° , respectively, and the dihedral angles among the three phenyl rings B and C, B and D, and C and D are 80.00° , 49.44° and 35.55° , respectively (Fig.4c). These dihedral data indicate that the TCPB^{3-} ligand is extremely unsymmetrical and the phenyl rings in TCPB^{3-} are not coplanar so as to satisfy the coordination geometry of Co^{2+} . The bond lengths of Co-O bond distances range from 0.202 78(16) to 0.221 48 (16) nm, and the O-Co-O bond angles span from 60.16° to 177.02° (Table S2), which are

compatible with the values of the previously published reports in literatures^[36]. The carboxylate groups in complex **2** adopt chelating and bidentate bridging coordination modes to coordinate with three Co ions to form a three-nuclear Co cluster unit $[\text{Co}_3(\text{COO})_6]$ SBU. Overall, as shown in Fig.4c and 4d, each TCPB^{3-} ligand connects three $[\text{Co}_3(\text{COO})_6]$ SBUs and each $[\text{Co}_3(\text{COO})_6]$ SBU is surrounded by six TCPB^{3-} ligands, generating a two-dimensional (2D) net-like layered framework (Fig.4e and S4). From the view point of topology, the 2D structure of **2** can be described as a (3,6)-connected network with Schflfi symbol of $\{4^3\}_4 \cdot \{4^6 \cdot 6^{18} \cdot 8^4\}$ by considering each $[\text{Co}_3(\text{COO})_6]$ SBU as a 6-connected node and the organic ligand TCPB^{3-} as a 3-connected node (Fig.2f).

2.2 Thermal analysis

The thermal stability of **1** and **2** were also detected via thermogravimetric analyses (TGA). The thermal analyses of powdered samples of **1** and **2** were performed under a nitrogen atmosphere. As shown in Fig.5, complex **1** lost three guest water molecules and one guest DMF molecule from room temperature to 200 °C (Obsd. 9.11%, Calcd. 8.78%), while complex **2** was stable up to 105 °C and then exhibited one step of weight loss. The weight loss of 22.11% (Calcd. 22.28%) in the temperature range of 105 ~210 °C corresponds to the release of one guest DMF molecule, one coordinated DMF molecule and one coordinated water molecule. After the guest and the coordinated solvent molecules are removed, a plateau appears and the desolvated sample was thermally stable up to 290 °C for **1** and 450 °C for **2**. Above 290

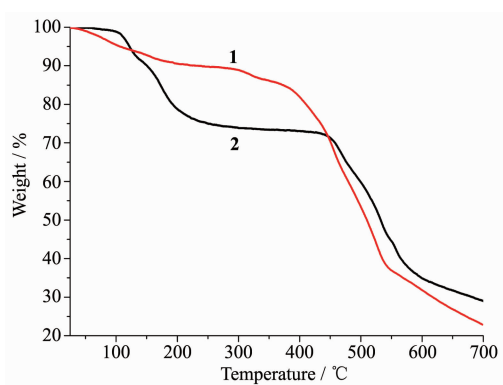


Fig.5 TG curves of **1** and **2**

°C for **1** and 450 °C for **2**, the framework gradually began to break down with the decomposition of the organic part of framework. From the decomposition temperature shown above, complex **2** exhibits good thermal stability. This may be attributed to the coordinatively linked net-like structure.

2.3 Photoluminescence property

The solid-state photoluminescent properties of complex **1** and **2** together with H_3TCPB and 4,4'-BPY were investigated at room temperature. As depicted in Fig.6, the H_3TCPB ligand exhibited only a broad emission band with a maximum at 354 nm upon excitation with $\lambda_{\text{ex}}=280$ nm (the excitation spectra is presented in Fig.S5), and 4,4'-bipyridine ligand showed an intense band centered at 466 nm, together with a broad and weak emission band located around 361 nm under the excitation at 300 nm, which may be caused by the $\pi^*-\pi$ and π^*-n transition. As for complex **1**, upon excitation at 320 nm, it showed blue luminescence (Fig.7) with a large broad band emission centered at 465 nm and a weak emission at 361 nm (Fig. 6, and the excitation spectra is given in Fig.S6). As the literature reported, the d^{10} configured Zn(II) cations are electrochemically inert, therefore, when coordinated by ligands, they cannot take an electron from the ligand with their 3d-orbitals, nor donate an electron to the ligand^[37]. In contrast to the emission of the free ligands, the emission band of **1** exhibited red-shifted as compared to free H_3TCPB ligand, and was close to the free 4,4'-BPY ligand, inferring that its emission bands may be assigned to the intra-ligand

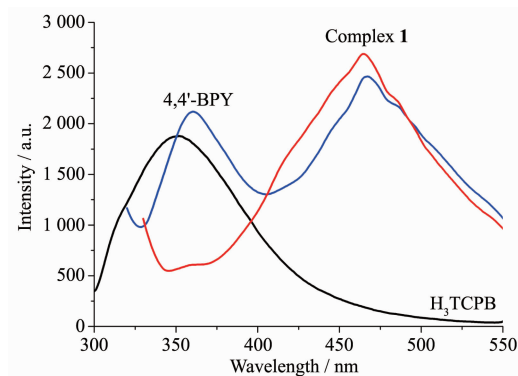


Fig.6 Emission spectra of **1**, 4,4'-BPY and H_3TCPB ligand in solid state at room temperature

charge transfer (ILCT), neither metal-to-ligand charge transfer (MLCT) nor ligand-to-metal charge transfer (LMCT) happened^[38]. Moreover, the red-shift of the intense emission in **1** could be attributed to the coordination effect, which affects the HOMO and LUMO levels of the ligand to change the transition energy, and enables the rigidity of the aromatic backbones and reduces the loss of energy by radiationless decay of the intraligand emissions^[39]. However, experimental results showed that complex **2** was non-emissive under similar conditions, indicating that the emissions of organic ligands may be quenched completely in the complex, which may be due to the emission quencher of Co(II) in the structure^[38].

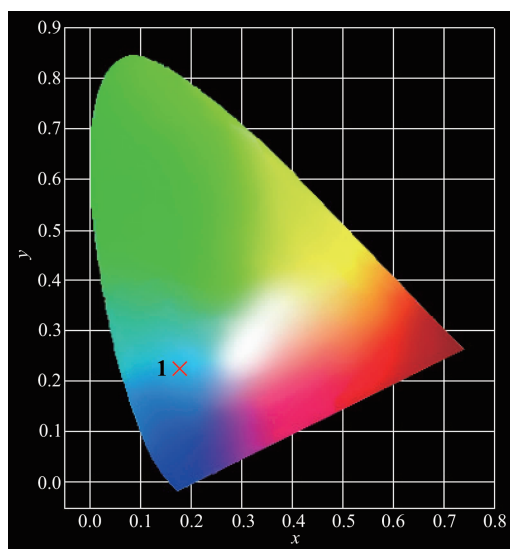


Fig.7 CIE chromaticity diagram for **1**

3 Conclusions

In summary, two novel MOFs, $\{[\text{Zn}_3(\text{TCPB})_2(4,4'\text{-BPY})]\cdot\text{DMF}\cdot 3\text{H}_2\text{O}\}_n$ (**1**) and $\{[\text{Co}_{1.5}(\text{TCPB})(\text{DMF})(\text{H}_2\text{O})]\cdot\text{DMF}\}_n$ (**2**) (H_3TCPB = 1,3,5-tri (4-carboxyphenoxy) benzene), have been successfully synthesized via solvothermal reactions. Complex **1** possesses a three-dimensional net framework constructed by three-nuclear zinc SBUs, TCPB³⁻ and 4,4'-BPY linker. Complex **2** has a 2D layered structure constructed by trinuclear cobalt cluster as SBUs. The solid-state photoluminescent property of **1** was investigated, and the emission band was assigned to the intra-ligand charge transfer (ILCT).

Acknowledgments: The authors thank National Nature Science Foundation of China for financial support (Grants No. 21371091, 21371150).

Supporting information is available at <http://www.wjhxxb.cn>

References:

- [1] (a) He H M, Sun F X, Zhao N, et al. *RSC Adv.*, **2014**, *4*:21535-21540
(b) WANG Peng-Fei(汪鹏飞), WU Xiao-Shuo(吴小说), WEI Bo(魏博), et al. *Chinese J. Inorg. Chem.*(无机化学学报), **2014**, *30*(7):1511-1517
- [2] (a) Yuan X, Zhang X, Zhao H, et al. *Cryst. Growth Des.*, **2013**, *13*:4859-4867
(b) YANG Long(杨龙), WANG Qin(王秦), DENG Yong-Jun(邓勇军), et al. *Chinese J. Inorg. Chem.*(无机化学学报), **2018**, *34*(7):1199-1208
- [3] (a) Jie D, Zou G L. *Inorg. Chem. Commun.*, **2016**, *69*:20-23
(b) HU Yun-Xia(胡云霞), ZHANG Wen-Wei(章文伟), WANG Li-Feng(王立锋), et al. *Chinese J. Inorg. Chem.*(无机化学学报), **2013**, *29*(7):1471-1479
- [4] (a) Zhang L, Yang W B, Wu X Y, et al. *Inorg. Chem. Commun.*, **2016**, *67*:10-13
(b) WANG Fu-Xue(王弗学), WANG Chong-Chen(王崇臣), WANG Peng(王鹏), et al. *Chinese J. Inorg. Chem.*(无机化学学报), **2017**, *33*(5):713-737
- [5] Song X Z, Song S Y, Zhang H J. *Struct. Bond.*, **2015**, *163*:109-144
- [6] Ma D X, Li B Y, Zhou X J, et al. *Chem. Commun.*, **2013**, *49*:8964-8966
- [7] Banerjee M, Das S, Yoon M, et al. *J. Am. Chem. Soc.*, **2009**, *131*:7524-7525
- [8] Qin Y H, Huang L, Zheng J X, et al. *Inorg. Chem. Commun.*, **2016**, *72*:78-82
- [9] Bigdeli F, Abedi S, Monfared H H, et al. *Inorg. Chem. Commun.*, **2016**, *72*:122-127
- [10] Wang C, Liu D, Lin W. *J. Am. Chem. Soc.*, **2013**, *135*:13222-13234
- [11] He Y P, Tan Y X, Zhang J. *Inorg. Chem.*, **2013**, *52*:12758-12762
- [12] Wu J X, Yan B. *Inorg. Chem. Commun.*, **2016**, *70*:189-192
- [13] Chen D M, Tian J Y, Liu C S. *Inorg. Chem. Commun.*, **2016**, *68*:29-32
- [14] Wang Y P, Li X Y, Li H H, et al. *Inorg. Chem. Commun.*, **2016**, *70*:27-30
- [15] Wang H H, Zhou L J, Wang Y L, et al. *Inorg. Chem. Commun.*, **2016**, *73*:94-97

- [16]Cui Y J, Yue Y F, Qian G D, et al. *Chem. Rev.*, **2012**,**112**: 1126-1162
- [17]Zhu M, Li M T, Zhao L, et al. *Inorg. Chem. Commun.*, **2017**, **79**:69-73
- [18]Pan Z R, Zheng H G, Wang T W, et al. *Inorg. Chem.*, **2008**, **47**:9528-9536
- [19]Zhang M D, Di C M, Zheng H G. *Inorg. Chem. Commun.*, **2013**,**27**:88-91
- [20]Xu H B, Zhou S H, Xiao L L, et al. *J. Mater. Chem. C*, **2015**,**3**:291-297
- [21]Dong X Y, Wang R, Wang J Z, et al. *J. Mater. Chem. A*, **2015**,**3**:641-647
- [22]Chen M, Wang Z W, Zhao H, et al. *Inorg. Chem. Commun.*, **2014**,**45**:84-88
- [23]Hassan M, Haque E, Reddy K R, et al. *Nanoscale*, **2014**,**6**: 11988-11994
- [24]Zhao S N, Su S Q, Song X Z, et al. *Cryst. Growth Des.*, **2013**,**13**:2756-2765
- [25]Fan L, Zhang X, Sun Z, et al. *Cryst. Growth Des.*, **2013**,**13**: 2462-2475
- [26]Deng Z P, Zhang Z Y, Huo L H, et al. *CrystEngComm*, **2012**,**14**:6548-6558
- [27]Kan W Q, Ma J F, Liu B, et al. *CrystEngComm*, **2012**,**14**: 286-299
- [28]Yan C, Fan Y Z, Chen L, et al. *CrystEngComm*, **2015**,**17**: 546-552
- [29]Zhai Q G, Zeng R R, Li S N, et al. *CrystEngComm*, **2013**, **15**:965-976
- [30]Chaudhari A K, Nagarkar S S, Joarder B, et al. *Cryst. Growth Des.*, **2013**,**13**:3716-3721
- [31]APEX 2, SAINT, XPREP, Bruker AXS Inc., Madison, Wisconsin, USA, **2007**.
- [32]SADABS, Bruker AXS Inc., Madison, Wisconsin, USA, **2001**.
- [33]Sheldrick G M. *SHELXS-97* and *SHELXL-97*, University of Göttingen, Germany, **1997**.
- [34]Spek A L. *J. Appl. Crystallogr.*, **2003**,**36**:7-13
- [35]Zhang J, Yang W B, Wu X Y, et al. *Cryst. Growth Des.*, **2016**,**16**:475-482
- [36]Chen M, Zhao H, Liu C S, et al. *Chem. Commun.*, **2015**,**51**: 6014-6017
- [37]Kan W Q, Ma J F, Liu Y Y, et al. *CrystEngComm*, **2012**,**14**: 2316-2326
- [38]Gao Y P, Guo L, Dong W, et al. *J. Solid State Chem.*, **2016**, **240**:82-90
- [39]Robin A Y, Fromm K M. *Coord. Chem. Rev.*, **2006**,**250**:2127-2157